

# The quenched trap model on the extreme landscape: the rise of sub-diffusion and non-Gaussian diffusion

Liang Luo<sup>1,2</sup> and Ming Yi<sup>3,\*</sup>

<sup>1</sup>*Department of Physics, Huazhong Agricultural University, Wuhan 430070, China*

<sup>2</sup>*Institute of Applied Physics, Huazhong Agricultural University, Wuhan 430070, China*

<sup>3</sup>*School of Mathematics and Physics, China University of Geosciences, Wuhan 430074, China*

Non-Gaussian diffusion has been intensively studied in recent years, which reflects the dynamic heterogeneity in the disordered media. The recent study on the non-Gaussian diffusion in a static disordered landscape suggests novel phenomena due to the quenched disorder. In this work, we further investigate the random walk in this landscape under various effective temperature  $\mu$ , which continuously modulates the dynamic heterogeneity. We show in the long time limit, the trap dynamics on the landscape is equivalent to the quenched trap model, in which sub-diffusion appears for  $\mu < 1$ . The non-Gaussian distribution of displacement has been analytically estimated for short  $t$ , of which the stretched exponential tail is expected for  $\mu \neq 1$ . Due to the localization in the ensemble of trajectory segments, an additional peak arises in  $P(x, t)$  around  $x = 0$  even for  $\mu > 1$ . Evolving in different time scales, the peak and the tail of  $P(x, t)$  are well split for a wide range of  $t$ . This theoretical study reveals the connections among the sub-diffusion, non-Gaussian diffusion, and the dynamic heterogeneity in the static disordered medium. It also offers an insight on how the cell would benefit from the quasi-static disordered structures.

## I. INTRODUCTION

Dynamic heterogeneity[1–3] has been recognized as the key feature of glassy systems, which refers to the widely spanned relaxation time of the disordered structures, the highly intermittent particle dynamics, and the large trajectory-to-trajectory fluctuations. The non-Gaussian diffusion, of which the distribution of particle displacement is not Gaussian, is observed in a wide range of disordered systems with dynamic heterogeneity, including the crowding intracellular environments[4–7], colloidal[8, 9] and granular[10] systems.

A simple interpretation reveals the connection between the dynamic heterogeneity and the non-Gaussian diffusion by modeling the heterogeneity with the random instantaneous diffusivity  $D^{(t)}$ [8, 11].  $P(x, t)$  is hence a convolution over  $D^{(t)}$  by

$$P(x, t) = \int dD^{(t)} G(x, t|D^{(t)})P(D^{(t)}), \quad (1)$$

where  $G(x, t|D^{(t)})$  is the Gaussian kernel for the short segment with the given  $D^{(t)}$ . Chubynsky and Slater[12] constructed the dynamics by setting the diffusivity itself an Ornstein-Uhlenbeck process, which is hence temporal correlated. The non-Gaussian behavior exists in the correlation time scale. The recent studies on the diffusion with fluctuating diffusivity[13–17] have largely improve our understanding on the non-Gaussian diffusion in the annealed disordered environments, where the relaxation time of the environments are assumed in the same scale of the particle diffusion and no spatial structure is considered.

The annealed assumption may fail, however, when the disordered environments are greatly influenced by the large structures in the media, such as the actin under the cell membrane[18, 19] or endoplasmic reticulum in the cytoplasm[20]. In the case that the structures fluctuate quite slow, the disordered sample is quasi-static[6, 7, 20–23] over the whole experiment. To investigate the non-Gaussian diffusion in such case, we have recently constructed a spatially correlated random landscape by a trick from extreme statistics[24, 25]. Employing the trap dynamics on the landscape with fixed temperature  $\mu = 1$ , we have discovered novel phenomena on non-Gaussian diffusion, which are unique for the quenched disorder.

In this work, we further investigate the trap dynamics on the “extreme landscape” of different heterogeneous levels, which are continuously modulated by the effective temperature  $\mu$ . A coarse-graining process is introduced to handle the spatial correlation in the landscape, via which the equivalence between the current model and the quenched trap model (QTM) with no spatial correlation[26–29] are revealed in the long time limit. A transition to sub-diffusion arises due to strong heterogeneity when  $\mu < 1$ . In this quenched case, a localization happens in the ensemble of the trajectory segments. A peak in  $P(x, t)$  around  $x = 0$  arises accordingly, which is significantly split from the stretched exponential tail.

The paper is organized as follows. In Sec. II, we introduce the extreme landscape and show how the effective temperature of the trap dynamics controls the heterogeneity. In Sec. III, we introduce a coarse-graining process, which connects the current model to the traditional QTM. In Sec. IV, we investigate the structure of the non-Gaussian distribution of displacement. Sec.V discusses the biological implication of the results and their connections with other works. A short summary follows in Sec. VI.

---

\* yiming@mail.hzau.edu.cn

## II. THE TRAP DYNAMICS ON THE EXTREME LANDSCAPE

We consider the random walk on a static disordered landscape  $\{V_i\}$  in two-dimensional cubic lattice, where  $i$  denotes the lattice site. The landscape was proposed to record the information of local minima of random auxiliary landscapes. It can be called the ‘‘extreme landscape’’. The generation of the extreme landscape  $\{V_i\}$  typically follows two steps:

1. Generate an auxiliary uncorrelated random landscape  $\{U_i\}$ , following the exponential distribution

$$P(U_i = U) = U_0^{-1} \exp(U/U_0), \quad U < 0. \quad (2)$$

2. Assign  $V_i$  by the local minimum of  $\{U_i\}$  in the  $r_c$ -neighbourhood of site  $i$ , i.e.,

$$V_i = \min \{U_j | r_{ij} < r_c\}. \quad (3)$$

Noting that the auxiliary landscape  $\{U_i\}$  is uncorrelated,  $P(V_i = V)$  converges to the limit distribution of extreme statistics for  $r_c^2 \gg 1$ , which distribution is known as the Gumbel distribution

$$P(V_i = V) = \exp[V - V_0 - \exp(V - V_0)]. \quad (4)$$

The extreme landscape is essentially determined by spatial distribution of the local minima of the auxiliary landscape. Each minimum dominates a range of the neighbour traps, which shape a basin of radius  $r_c$  in the extreme landscape. The extreme landscape is constituted by the overlapped extreme basins (See Fig.1 in [25]). It is hence locally correlated up to  $2r_c$ .

In this work, the trap dynamics is employed for the random walk on the extreme landscape. The escaping rate from the trap  $i$  is determined by the trap depth  $V_i$  by

$$w_i = w_0 \exp(V_i/\mu), \quad (5)$$

where  $V_i < 0$  for traps, the dynamical parameter  $w_0$  gives the time scale. The effective temperature  $\mu$  controls the roughness of the landscape and hence the spatial heterogeneity of the dynamics. The typical sojourn time in trap  $i$  can be estimated by

$$\tau_i = w_i^{-1} = w_0^{-1} \exp(-V_i/\mu). \quad (6)$$

In trap dynamics, the particle at site  $i$  jumps to all the nearest-neighbour sites  $j$  with even rate  $w_{i \rightarrow j} = n_c^{-1} w_i$ , where  $n_c = 4$  is the coordination number in square lattice. The local diffusivity at site  $i$  can be hence defined as

$$D_i^{(l)} \equiv \frac{a^2}{4\tau_i} = \frac{w_0 a^2}{4} \exp(V_i/\mu), \quad (7)$$

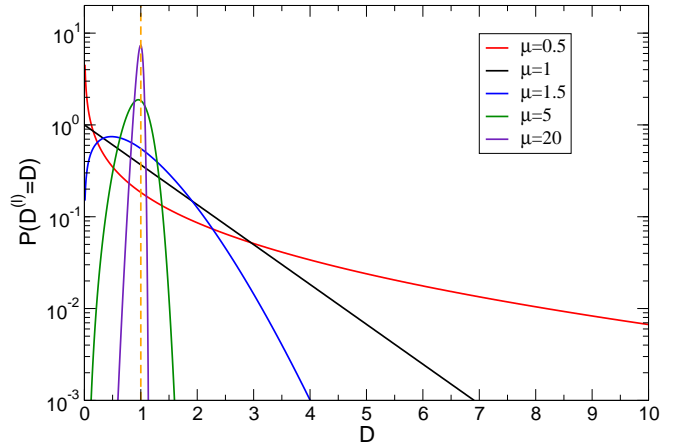


FIG. 1. The distribution of local diffusivity for various  $\mu$ , given by Eq.(8).

Noting that  $\{V_i\}$  follows the Gumbel distribution given by Eq.(4), one can see  $\{D_i^{(l)}\}$  follows the generalized Gamma distribution with a stretched exponential tail

$$P(D_i^{(l)}/D_0 = D) = \mu D^{\mu-1} \exp(-D^\mu), \quad (8)$$

where  $D_i^{(l)}$  is scaled by  $D_0 = w_0 a^2 \exp(V_0/\mu)/4$ . Noting  $V_0 < 0$ , one can see  $D_0$  vanishes in the low temperature cases with  $\mu \ll 1$ , where the walk in the media is frozen. To exclude the freezing effects and to focus on the spatial heterogeneity, we rescale the landscape in this work by setting  $D_0 = 1$ . The mean value of  $D^{(l)}$  then moderately depends on  $\mu$  by  $\langle D^{(l)} \rangle = \mu^{-1} \Gamma(\mu^{-1})$ , where  $\Gamma(\cdot)$  is the Gamma function. For intuition,  $0.88 < \langle D^{(l)} \rangle < 2$  for any  $\mu > 0.5$ . Figure 1 shows the distribution of the rescaled local diffusivity,  $P(D^{(l)})$ , for some typical temperatures. In the high temperature limit,  $\mu \rightarrow \infty$ ,  $P(D_i^{(l)}/D_0 = D)$  converges to a peak around  $D = 1$ . The dynamics hence degenerates to the normal Brownian motion in the homogeneous media. For  $\mu = 1$ , Eq.(8) turns to  $P(D_i^{(l)}/D_0 = D) = \exp(-D)$ , which has been previously studied[25] as a special case of non-Gaussian diffusion with the exponential tail.

## III. THE COARSE-GRAINING PROCESS AND THE LONG-TIME BEHAVIOR

In this section, we introduce the coarse-graining (CG) process for the trap model to handle the local correlation in the landscape. Considering a sample of finite size and periodic boundaries, the random walk can scan all the traps of the sample in the long time limit. The diffusion process achieves a steady state, of which the mean squared displacement  $\langle |\Delta x(t)|^2 \rangle = \langle |x(t) - x(0)|^2 \rangle$  can be written by

$$\langle |\Delta x(t)|^2 \rangle = 4D_{\text{dist}}, \quad \text{for } t \rightarrow \infty. \quad (9)$$

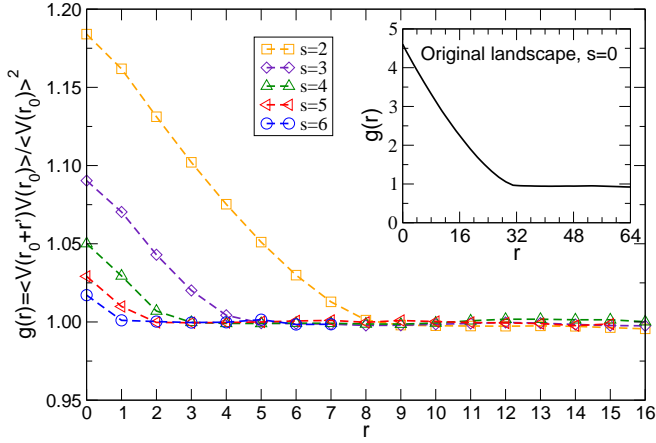


FIG. 2. The pair correlation function  $g(r)$  of the coarse-grained landscapes at various CG levels  $s$ . The radius of the extreme basin is set by  $r_c = 16$ . The inset shows  $g(r)$  of the original extreme landscape.

One can show in trap dynamics that the diffusion coefficient  $D_{\text{dis}}$  depends on the mean sojourn time[26, 27, 30] by

$$D_{\text{dis}} = a^2/4\bar{\tau}, \quad (10)$$

where the mean sojourn time  $\bar{\tau}$  averages over the traps in the sample by

$$\bar{\tau} = \frac{1}{N} \sum_{i=1}^N \tau_i. \quad (11)$$

Sharing the spirit with Machta's early work[31] on QTM, we regroup the summands in Eq.(11) by blocks of neighbours. It leads the CG operation as follows:

1. In a lattice of  $N$  sites, we replace each  $2 \times 2$  block by a single site on a lattice of  $N' = N/4$  sites and the lattice constant  $a' = 2a$ .
2. To keep the sum of all the  $\tau_i$  invariant, the typical sojourn time  $\tau'_q$  in a coarse-grained site  $q$  is set the sum of those in the original block,

$$\tau'_q = \sum_{j \in \text{block } q} \tau_j, \quad (12)$$

where  $\tau_j$  is the typical waiting time of the  $j$ th site in block  $q$ .

Repeating the operation for  $s$  times, we achieve a landscape of CG level  $s$ , which is constituted by  $N^{(s)} = N/4^s$  traps. The mean sojourn time of the coarse-grained landscape is given by

$$\overline{\tau^{(s)}} = \frac{1}{N^{(s)}} \sum_{q=1}^{N^{(s)}} \tau_q^{(s)} = 4^s \bar{\tau}, \quad (13)$$

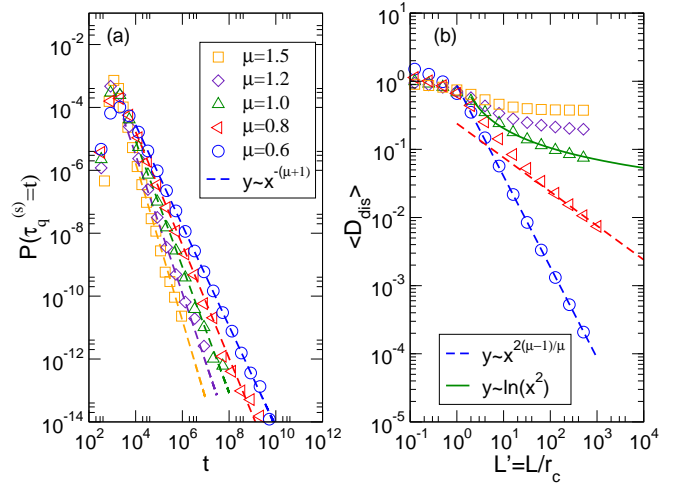


FIG. 3. (a) The probability density function of the sojourn time in the traps of the coarse-grained landscape with the CG level  $s = 6$  from simulations for various  $\mu$ . (b) The size dependence of  $\langle D_{\text{dis}} \rangle$ , where the lattice size is rescaled by the correlation length  $r_c$ . The symbols denote the numerical results for various  $\mu$ , as the same in (a).

where  $\tau_q^{(s)}$  denote the typical sojourn time in the  $q$ th trap. Noting that the lattice constant  $a^{(s)} = 4^s a$ , we see the diffusion coefficient  $D_{\text{dis}}^{(s)} = (a^{(s)})^2 / (4\overline{\tau^{(s)}})$  is invariant over coarse-graining. On the other hand, the spatial correlation quits the coarse-grained landscape, as shown by the pair correlation function of the effective landscape  $\{\tilde{V}_q^{(s)} \equiv -\ln \tau_q^{(s)}\}$  in Fig.2. One can clearly read the decline of the correlation, which vanishes when the grain size  $l = 2^s$  is larger than the diameter of the extreme basin  $2r_c$ .

Figure 3(a) shows the probability density function of the typical sojourn time in traps,  $\{\tau_q^{(s)}\}$ , of the fully coarse-grained landscapes. One can clearly read the power-law tails contributed by the sojourn time in the deepest traps. Being more precise, the depth of the original traps follows the Gumbel distribution given by Eq.(4), of which the tail is merely exponential shaped. The exponential tail of  $P(V_i)$  leads to the power-law tail of sojourn time distribution. It recalls to us the intensively studied QTM with no spatial correlation, in which the heavy-tailed sojourn time distribution leads to sub-diffusion.

Sub-diffusion does arise in trap dynamics on the extreme landscape when  $\mu \leq 1$ . In the rest of the section, we characterize the sub-diffusive behavior by the size dependence of diffusion coefficient  $D_{\text{dis}}$  of the extreme landscape in a brief way. For more technical details, one can go to the classical reviews[26, 27] and also the recent papers[29, 30, 32].

Sub-diffusion refers the sub-linear time dependence of MSD, where  $D_{\text{dis}}$  vanishes as the particle scans broader range of the sample. The QTM captures the feature of sub-diffusion by the size dependence of  $D_{\text{dis}}$ , which is

connected to the mean sojourn time of the sample via Eq.(10). For simplicity, we consider the fully coarse-grained landscape with  $M = N^{(s)} = N/4^s$  traps, where  $\{\tau_q^{(s)}\}$  is independently and identically distributed. In the case that the distribution of  $\tau_q^{(s)}$  is with a power-law tail,  $P(\tau_q^{(s)} = t) \sim ct^{-(\mu+1)}$ , one may note a random energy model (REM) like transition[33, 34] happens for  $\mu < 1$ , where the summation of  $\tau_q^{(s)}$  in Eq.(13) is dominated by the largest summand. Including more terms in the summation, the typical value of the largest  $\tau_q^{(s)}$  increases as  $\tau_{\text{typ}} \sim M^{1/\mu}$ , which is faster than linear. The mean sojourn time  $\overline{\tau^{(s)}}$  hence diverges for large  $M$ . The vanishing  $D_{\text{dis}}$  becomes the consequence. The generalized CLT suggests the rescaled summation of  $\tau_q^{(s)}$  follows the one-sided Lévy stable distribution by

$$\frac{A}{M^{1/\mu}} \sum_{q=1}^M \tau_q^{(s)} \equiv \tilde{\tau} \sim L_\mu, \text{ for } \mu < 1, \quad (14)$$

where the normalization parameter  $A$  depends on  $\mu$  and  $c$ . Noting  $\overline{\tau^{(s)}} = A^{-1}M^{\frac{1-\mu}{\mu}}\tilde{\tau}$  and also  $D_{\text{dis}} = (a^{(s)})^2/(4\overline{\tau^{(s)}})$ , one can estimate the mean diffusion coefficient averaged over samples by

$$\langle D_{\text{dis}} \rangle = M^{1-\frac{1}{\mu}} \frac{(a^{(s)})^2}{4} A \langle \tilde{\tau}^{-1} \rangle, \quad (15)$$

and the sample-to-sample fluctuation by

$$\langle |D_{\text{dis}} - \langle D_{\text{dis}} \rangle|^2 \rangle = M^{2-\frac{2}{\mu}} \frac{(a^{(s)})^4}{16} A^2 \left[ \langle \tilde{\tau}^{-2} \rangle - \langle \tilde{\tau}^{-1} \rangle^2 \right], \quad (16)$$

where the negative moments[35] of  $\tilde{\tau}$  depend only on  $\mu$ . Noting  $M = (L/2^s)^2$ , one can see  $\langle D_{\text{dis}} \rangle \propto L^{2(\mu-1)/\mu}$  for  $\mu < 1$ . In the marginal  $\mu = 1$  case, the logarithmic size dependence,  $\langle D_{\text{dis}} \rangle \propto 1/\ln L^2$ , has been reported in the previous work[25]. For higher  $\mu$ , the mean value of  $\tau_q^{(s)}$  exists. Self-averaging can be achieved in large samples.  $\langle D_{\text{dis}} \rangle$  hence converges to a finite value. In other words, the random walk in less heterogeneous landscapes with  $\mu > 1$  return to the normal Brownian motion in the long time limit. Our simulation confirms the above results on size dependences of  $D_{\text{dis}}$  for various  $\mu$ , as shown in Fig.3(b).

#### IV. NON-GAUSSIAN DIFFUSION WITH THE STRETCHED EXPONENTIAL TAIL AND THE PEAK AROUND $x = 0$

In this section, we investigate the distribution of displacement of random walk on the extreme landscape. In practice of data analysis, the distribution of displacement  $P(x, t)$  is usually obtained by counting the head-to-tail displacement  $x$  of trajectory segments of time duration  $t$ . In this work, we generate the trajectories by the kinetic

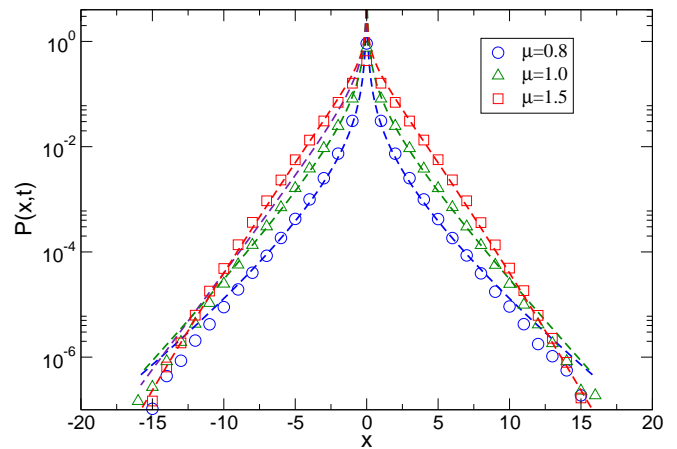


FIG. 4. The distribution of displacement  $P(x, t)$  for  $t = 2.5$  and various  $\mu$  and  $t$  in a typical disordered sample. The symbols are obtained from simulations and the dash lines are given according to Eq.(21).

Monte Carlo simulation, of which the random walk is defined by the nearest-neighbour hopping rate  $w_{i \rightarrow j} = w_i/4$  and the escaping rate  $w_i = w_0 \exp(V_i/\mu)$ . The size of the disordered samples  $\{V_i\}$  are chosen as  $L_x = L_y = 1024$ , while the radius of the extreme basin is set as  $r_c = 16$ . The periodic boundary condition is also applied. To simulate the fully equilibrium case, the initial positions of the walk are randomly generated following the Boltzmann distribution, i.e.  $P_i \propto \tau_i = a^2/4D_i^{(l)}$ .

Figure 4 shows  $P(x, t)$  obtained from short segments with  $t = 2.5$  and various  $\mu$ . In the short segments, the particles rarely walk out of the origin extreme basin. The instantaneous diffusivity of the segments  $D^{(t)}$  can be hence approximated by the local diffusivity  $D^{(l)}$  of the extreme basin. Given the origin site  $i$  of a short segment, one can expect the displacement of the segment follows the Gaussian distribution governed by a single diffusivity  $D^{(t)} = D_i^{(l)}$  as

$$G(x, t|D^{(t)}) = \frac{1}{\sqrt{4\pi D^{(t)}t}} \exp\left(-\frac{x^2}{4D^{(t)}t}\right). \quad (17)$$

Counting all the segments of various  $D^{(t)}$ ,  $P(x, t)$  follows a convolution

$$P(x, t) = \int_0^\infty dD^{(t)} G(x, t|D^{(t)}) P(D^{(t)}|D_{\text{dis}}), \quad (18)$$

where  $P(D^{(t)}|D_{\text{dis}})$  is the distribution of the instantaneous diffusivity, recording the local diffusivity of the extreme basin visited by each short segment. Noting in the equilibrium state the segments sample the landscape with the Boltzmann weight, one can see

$$P(D^{(t)} = D|D_{\text{dis}}) = \sum_i P(D_i^{(l)} = D|D_{\text{dis}}) P(x_i|D_i^{(l)}, D_{\text{dis}}), \quad (19)$$

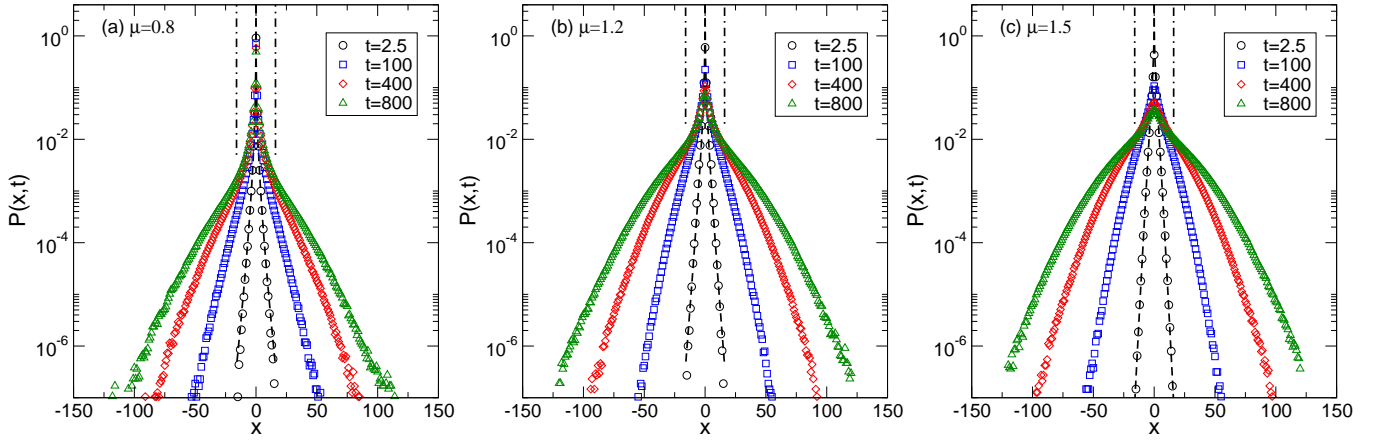


FIG. 5. The time-dependence of distribution of displacement  $P(x, t)$  in a typical disordered sample for (a)  $\mu = 0.8$ , (b)  $\mu = 1.2$ , and (c)  $\mu = 1.5$ . The symbols are obtained from simulations and the black dash lines are given according to Eq.(21). The radius of the extreme basin  $r_c = 16$  is marked by dash-dot lines for guidance.

where  $P(x_i|D_i^{(l)}, D_{\text{dis}})$  is the Boltzmann weight of trap  $i$  in the sample with  $N$  traps. Employing Eq.(7), Eq.(10) and Eq.(11), it can be explicitly written by

$$P(x_i|D_i^{(l)}, D_{\text{dis}}) = \frac{\tau_i}{\sum_{j=1}^N \tau_j} = \frac{D_{\text{dis}}}{ND_i^{(l)}}. \quad (20)$$

Noting Eq.(8), one can see Eq.(18) is indeed a convolution of the generalized Gamma distribution and the Gaussian distribution. Sposini *et al.*[16] offers several approaches for the estimation of the convolution. In the Appendix of this paper, a saddle point approach is introduced, which gives the correct large- $x$  asymptotic behavior by

$$P(\tilde{x}, t) \approx \frac{1}{\sqrt{4t}} AD_{\text{dis}} \tilde{x}^{(\mu-3)/(\mu+1)} \exp\left[-B\tilde{x}^{2\mu/(1+\mu)}\right], \quad (21)$$

where  $\tilde{x} = \sqrt{x^2/4t}$ , the prefactors  $A$  and  $B$  depend only on  $\mu$ . For the  $\mu = 1$  case, it returns to the simple expression  $P(x, t|D_{\text{dis}}) = D_{\text{dis}}x^{-1} \exp(-x/\sqrt{t})$ , which has been obtained in [25]. For the  $\mu \neq 1$  cases, the stretched/shrunk exponential tail is suggested by Eq.(21), which is confirmed by the simulations as shown in Fig.4. It is a bit surprising that the asymptotic expression (Eq.(21)) works even to very small  $x$ , where a peak  $P(x) \sim (x^2/4t)^{(\mu-3)/(2\mu+2)}$  is expected. The peak is mainly contributed by the segments in the deepest traps of the sample, which are heavily weighted in the ensemble of segments. Noting the constraint  $P(x_i|D_i^{(l)}, D_{\text{dis}}) < 1$ , one can learn from Eq.(20) that the local diffusivity in a given sample is bounded by  $D^{(l)} > D_c \equiv D_{\text{dis}}/N$ . The height of the peak at  $x = 0$  is hence also bounded, which can be estimated as

$$P(x = 0, t|D_{\text{dis}}) \approx \frac{D_{\text{dis}}}{\sqrt{4\pi t}} \Gamma\left(\frac{2\mu-3}{2\mu}, D_c^\mu\right). \quad (22)$$

Here  $\Gamma(\alpha, z) = \int_z^\infty dt t^{\alpha-1} \exp(-t)$  is the incomplete Gamma function. In the case with  $\mu < 3/2$ ,

$\Gamma((2\mu-3)/2\mu, D_c^\mu) \sim D_c^{\mu-3/2}$  for small  $D_c$ , which diverges when  $D_c \rightarrow 0$ . It is interesting to note that  $P(D^{(l)} = 0) = 0$  for  $\mu > 1$  (see Fig.1). The sharp peak appearing in the  $1 < \mu < 3/2$  cases is purely from the localization in the ensemble of trajectory segments, which is a unique phenomenon in the static disordered media.

The above estimation based on the assumption that the short segments are dominated by single local diffusivity. This assumption is not suitable for longer  $t$ , in which case the particle may visit multiple extreme basins. Averaging over various  $D^{(l)}$  of the basins, the tail of  $P(x, t)$  for longer  $t$  gradually deviates from Eq.(21), as shown in Fig. 5. On the other hand, the peak contributed by the particles localized in the deepest basins relaxes in different time scale. The sharp peak persists for very long time in the sub-diffusive  $\mu = 0.8$  case, since a genuine glass transition (REM-like transition) drives the deepest trap away from the others. The waiting time in the deepest trap is magnitude larger than that in the others. In the diffusive  $1 < \mu < 3/2$  cases, the peak due to the localization in the ensemble of segments can still be identified from the tail even for very long  $t$ . The whole particle (segment) population are hence split into the “mobile” and “immobile” states, until the localized particle eventually escape from the extreme basin of the deepest traps. The size of the extreme basin hence gives a length scale separating the peak and the tail, which is marked in the  $P(x, t)$ s shown in Fig.5.

## V. DISCUSSION

The heterogeneity of the disordered media often introduces different dynamical states in the diffusion process. In the model of aged CTRW[36–39], a portion of particles are localized, which contribute a peak around  $x = 0$  in  $P(x, t)$ . The phenomenon of “population splitting” is hence reported, where the displacements of the “im-

mobile” and “mobile” particles are well split. Similar splitting has also been observed in the simulation reporting non-Gaussian diffusion[7], where  $P(x, t)$  is piecewise-fitted. In this work, due to the localization in the ensemble of segments,  $P(x, t)$  is naturally constituted by the non-Gaussian tail and the peak around  $x = 0$ . The tail and the peak split for large  $t$ , which can be roughly identified as the “immobile” and “mobile” states.

The “immobile” particles are believed playing a key role in biological functions, such as the transmembrane signaling. Recent biology study suggests that the actin structures under the cell membrane help the formation of signaling hot spots on the membrane, where the signaling protein tends to stay and work[19]. In this work, we show in the disordered media fixed by the large structures, the “immobile” state spontaneously appears due to the localization in the ensemble of segments, which is merely a consequence of the equilibrium Boltzmann distribution in the static landscape. It may provide a hint that how the cell benefits from the crowding of the membrane.

The tail of a non-Gaussian distribution of displacement is surely not necessary being in the exact exponential form. The distribution with the stretched exponential tail is the more common case. Sposini et al. [16] has extended two models of annealed disordered systems to investigate a class of non-Gaussian diffusion with stretched exponential tail. In their models, the instantaneous diffusivity follows the generalized Gamma distribution. We show in this work a class of generalized Gamma distributions (Eq.8) can be the direct consequence of the trap dynamics on the extreme landscape. The stretched exponential tail of  $P(x, t)$  hence appears in this case of static disorder.

We note in this work the extreme landscape is locally correlated. A coarse-graining process is hence introduced to eliminate the correlation. Since the tail of Gumbel distribution can be well approximated by an exponential one, the CG process eventually leads us to the celebrated QTM. The QTM with uncorrelated traps has been intensively studied since early 1980s[26, 31, 40, 41]. This successful model helps us understanding sub-diffusion in static disordered media[27–29, 42, 43]. The trap dynamics on the extreme landscape is hence a extension of QTM, of which the local structures introduces the non-Gaussian diffusion.

## VI. SUMMARY

In summary, we have investigated the trap dynamics on the “extreme” landscape, of which the heterogeneity can be continuously modulated by the effective temperature  $\mu$ . We show in long time limit the model is equivalent to the celebrated quenched trap model with no spatial correlation. Sub-diffusion in the extreme landscape is hence expected and confirmed in the low temperature region with  $\mu < 1$ . Our analytical study reveals the connection between the stretched exponential tail of  $P(x, t)$

and the dynamic heterogeneity. We note a localization mechanism in the ensemble of segments, which is a consequence of the equilibrium Boltzmann distribution on the static landscape. The “immobile” state hence arises, of which the particles are well split from the fast moving “mobile” particles. The population splitting can appear in the  $1 < \mu < 3/2$  cases, while the sub-diffusion is absent. It provides an insight on how the cell benefits from the quasi-static structure of the cell membrane.

## ACKNOWLEDGMENTS

We would like to thank Hui Li for constant inputs and challenges from the experiment side. This work is supported by National Natural Science Foundation of China (Grant No. 11705064, 11675060, 91730301), Fundamental Research Funds for the Central Universities (Grant No. 2662016QD005), and the Huazhong Agricultural University Scientific and Technological Self-innovation Foundation Program (Grant No.2015RC021).

### Appendix: The non-Gaussian tail of $P(x, t)$ for small $t$

In this section, we estimate the convolution of Eq.(18)

$$P(x, t) = \int_0^\infty dD^{(t)} G(x, t|D^{(t)})P(D^{(t)}|D_{\text{dis}}), \quad (\text{A.1})$$

where  $P(D^{(t)}|D_{\text{dis}})$  is determined by the distribution of local diffusivity  $P(D_i^{(l)} = D|D_{\text{dis}})$  and the Boltzmann weight  $P(x_i|D_i^{(l)}, D_{\text{dis}})$  via Eq.(19).

We note in any sample, the diffusion coefficient  $D_{\text{dis}}$  is determined by the configuration of  $\{D_i^{(l)}\}$ . Known  $D_{\text{dis}}$  of the sample,  $D^{(l)}$  is hence bounded by  $D_i^{(l)} > D_c \equiv D_{\text{dis}}/N$ , which can be read from the natural constraint  $P(x_i|D_i^{(l)}, D_{\text{dis}}) < 1$ . The analysis in the previous work (see Appendix B of [25]) suggests the conditional probability  $P(D_i^{(l)} = D|D_{\text{dis}})$  can be approximated by  $P(D_i^{(l)} = D)$  for  $D > D_c$ , which is provided by Eq.(8). Combining also Eq.(19) and Eq.(20), we can obtain the distribution of instantaneous diffusivity reported by the short segments

$$P(D_i^{(t)} = D|D_{\text{dis}}) \approx \begin{cases} 0, & D < D_c \\ D_{\text{dis}}\mu D^{\mu-2} \exp(-D^\mu), & D \geq D_c \end{cases}. \quad (\text{A.2})$$

The explicit expression of Eq.(18) is hence written as

$$P(x, t|D_{\text{dis}}) = \frac{D_{\text{dis}}}{\sqrt{4\pi t}} \int_{D_c}^\infty dD \mu D^{\mu-5/2} \exp\left(-D^\mu - \frac{x^2}{4Dt}\right). \quad (\text{A.3})$$

One may note the segments with small  $D$  hardly contribute to the non-Gaussian tail for  $x^2 \gg 4D_c t$ . In such case, the lower bound of the integral can be released to

$D_c = 0$ . Sposini *et al.*[16] have estimated the integral via the Fox  $H$ -function and other approaches. We provide a saddle point approach below, which also gives the correct large- $x$  behavior.

Let  $\tilde{x} = \sqrt{x^2/4t}$ ,  $\tilde{D} = D/\tilde{x}^2$ , and  $f(\tilde{D}) = \tilde{x}^{2\mu}\tilde{D}^\mu + 1/\tilde{D}$ . The concerned convolution can be written by

$$P(\tilde{x}, t|D_{\text{dis}}) = \frac{D_{\text{dis}}}{\sqrt{4\pi t}} \tilde{x}^{2\mu-3} \int_0^\infty d\tilde{D} \mu \tilde{D}^{\mu-\frac{5}{2}} \exp(-f(\tilde{D})). \quad (\text{A.4})$$

For  $\tilde{x}^2 \gg 1$ , the saddle point approximation suggests

$$P(\tilde{x}, t) \approx \frac{D_{\text{dis}}}{\sqrt{4\pi t}} \tilde{x}^{2\mu-3} \mu D_s^{\mu-\frac{5}{2}} \sqrt{\frac{\pi}{f''(D_s)}} \exp(-f(D_s)), \quad (\text{A.5})$$

where the saddle point  $D_s = (\mu)^{-1/(1+\mu)} \tilde{x}^{-2\mu/(1+\mu)}$  gives the minimum value of  $f(D)$  by

$$f(D_s) = (1 + \mu) \mu^{-\mu/(1+\mu)} \tilde{x}^{2\mu/(1+\mu)}, \quad (\text{A.6})$$

and also

$$f''(D_s) = (1 + \mu) \mu^{2/(1+\mu)} \tilde{x}^{6\mu/(1+\mu)}. \quad (\text{A.7})$$

One can hence gets

$$P(\tilde{x}, t) \approx \frac{1}{\sqrt{4t}} A D_{\text{dis}} \tilde{x}^{(\mu-3)/(\mu+1)} \exp[-B \tilde{x}^{2\mu/(1+\mu)}], \quad (\text{A.8})$$

where  $A = (1 + \mu)^{-\frac{1}{2}} \mu^{\frac{2}{1+\mu}}$  and  $B = (1 + \mu) \mu^{-\frac{\mu}{1+\mu}}$ .

- 
- [1] L. Berthier, *Physics* **4**, 42 (2011).  
[2] L. Berthier and G. Biroli, *Rev. Mod. Phys.* **83** 587 (2011).  
[3] T. R. Kirkpatrick and D. Thirumalai, *Rev. Mod. Phys.* **87** 183 (2015).  
[4] B. P. Parry *et al.*, *Cell* **156** 183 (2014).  
[5] W. He, H. Song, Y. Su, L. Geng, B. J. Ackerson, H. B. Peng and P. Tong, *Nat. Commun.* **7**, 11701 (2016).  
[6] M. C. Munder *et al.*, *eLife* **5**, e09347 (2016).  
[7] J.-H. Jeon, M. Javanainen, H. Martinez-Seara, R. Metzler and I. Vattulainen, *Phys. Rev. X* **6**, 021006 (2016).  
[8] S. C. Bae, B. Wang, J. Guan and S. Granick, *Proc. Natl. Acad. Sci.* **106**, 15160 (2009).  
[9] T. Sentjabskaja *et al.*, *Nature Comm.* **7** 11133 (2016).  
[10] B. Kou, *et al.*, *Nature* **551**, 360 (2017).  
[11] B. Wang, J. Kuo, S. C. Bae and S. Granick, *Nat. Mater.* **11**, 481 (2012).  
[12] M. V. Chubynsky and G. W. Slater, *Phys. Rev. Lett.* **113**, 098302 (2014).  
[13] T. Akimoto and E. Yamamoto, *Phys. Rev. E* **93**, 062109 (2016).  
[14] A. G. Cherstvy and R. Metzler, *Phys. Chem. Chem. Phys.* **18**, 23840 (2016).  
[15] E. Aurell and S. Bo, *Phys. Rev. E* **96**, 032140 (2017).  
[16] V. Sposini, A. V. Chechkin, F. Seno, G. Pagnini, and R. Metzler, *New J. Phys.* **20** 043044 (2018).  
[17] J. Slezak, R. Metzler, and M. Magdziarz, *New J. Phys.* **20** 023026 (2018).  
[18] N. L. Andrews *et al.* *Nature Cell Biol.* **10** 955 (2008).  
[19] T. Sungkaworn *et al.* *Nature* **550** 543 (2017).  
[20] H. Li, S.-X. Dou, Y.-R. Liu, W. Li, P. Xie, W.-C. Wang and P.-Y. Wang, *J. Am. Chem. Soc.* **137**, 436 (2015).  
[21] S. K. Ghosh, A. G. Cherstvy, R. Metzler, *Phys. Chem. Chem. Phys.* **17**, 1847 (2015).  
[22] B.-S. Lu, F. Ye, X. Xing, P. M. Goldbart, *Phys. Rev. Lett.* **108**, 257803 (2012).  
[23] J. Wang, Y. Zhang and H. Zhao, *Phys. Rev. E* **93**, 032144 (2016).  
[24] L. Luo and M. Yi, *Sci. China-Phys. Mech. Astron.* **59**, 120521 (2016).  
[25] L. Luo and M. Yi, *Phys. Rev. E* **97**, 042122 (2018).  
[26] J. W. Haus and K. W. Kehr, *Phys. Rep.* **150**, 263 (1987).  
[27] J. P. Bouchaud and A. Georges, *Phys. Rep.* **195**, 127 (1990).  
[28] S. Burov and E. Barkai, *Phys. Rev. Lett.* **106**, 140602 (2011).  
[29] L. Luo and L.-H. Tang, *Chin. Phys. B* **23**, 070514 (2014).  
[30] T. Akimoto, E. Barkai and K. Saito, *Phys. Rev. Lett.* **117**, 180602 (2016).  
[31] J. Machta, *J. Stat. Phys.* **30**, 305 (1983).  
[32] L. Luo and L.-H. Tang, *Phys. Rev. E* **92**, 042137 (2015).  
[33] B. Derrida, *Phys. Rev. B* **24**, 2613 (1981).  
[34] J.-P. Bouchaud and M. Mézard, *J. Phys. A: Math. Gen.* **30**, 7997 (1997).  
[35] A. V. Chechkin, M. Hofmann and I. M. Sokolov, *Phys. Rev. E* **80**, 031112(2009).  
[36] E. Barkai, *Phys. Rev. Lett.* **90**, 104101 (2003).  
[37] E. Barkai and Y.-C. Cheng, *J. Chem. Phys.* **118**, 6167 (2003).  
[38] J. H. P. Schulz, E. Barkai and R. Metzler, *Phys. Rev. Lett.* **110**, 020602 (2013).  
[39] J. H. P. Schulz, E. Barkai and R. Metzler, *Phys. Rev. X* **4**, 011028 (2014).  
[40] J. Machta, *Phys. Rev. B* **24**, 5260 (1981).  
[41] J. Machta, *J. Phys. A* **18**, L531 (1985).  
[42] C. Monthus, *Phys. Rev. E* **67**, 046109 (2003).  
[43] E. M. Bertin and J. P. Bouchaud, *Phys. Rev. E* **67**, 026128 (2003).